INVESTIGATIONS OF ISOLATION IMPROVEMENT TECHNIQUES FOR MULTIPLE INPUT MULTIPLE OUTPUT (MIMO) WLAN PORTABLE TERMINAL APPLICATIONS

H.-T. Chou, H.-C. Cheng, H.-T. Hsu, and L.-R. Kuo

Department of Communication Engineering
and Communications Research Center
Yuan Ze University
Chung-Li 320, Taiwan, R.O.C.

Abstract—Various isolation improvement techniques for MIMO WLAN card bus applications consisted of three closely spaced loop antennas are presented and investigated both numerically and experimentally in this paper. The proposed techniques are easily implemented and proven effective to achieve high isolation among the antennas which is a must for MIMO terminals to receive uncorrelated signals with good system throughputs.

1. INTRODUCTION

The rapid spread of internet has urged broad band communication access such as wireless local area networks (WLAN) and Worldwide Interoperability for Microwave Access (WiMAX) systems to be rigorously studied and actively implemented. From system point of view, increased data quantities and improved information quality have to be simultaneously achieved in order to meet the overwhelming demand in channel capacities. However, signal fading due to multipath propagation is an additional factor that may limit the system capacity. The use of multiple input multiple output (MIMO) system is one of the effective ways for improving reliability and increasing the capacity of the wireless channel [1–9]. Since the capacity of wireless channel is greatly affected by the mutual coupling between the antenna elements [10], antenna design for such systems plays a critical role because of the needs to exhibit distinguishable scattering characteristics among antennas in their specific radiating wave propagations. Furthermore, high isolation among antenna

elements is especially required for MIMO systems since this will guarantee the receipt of the uncorrelated signals when the antennas are closely spaced.

In general, for portable terminals, more than 2 antenna elements closely spaced in a restricted available space is usually the case and achieving high isolation without too much effort of additional elaboration is thus very challenging under such circumstances. Efforts [11–25] have been contributed to the reduction of mutual coupling between antennas. In [11], a smart antenna system consisted of microstrip antenna elements was presented. The reduction of mutual coupling between antenna elements were mainly achieved through proper design of the feeding network to the antenna elements. EBG (electromagnetic bandgap) periodic structures were placed in the vicinity of an antenna [12–15], which produced a band notch effect to prevent fields from penetrating through the structure to affect the antenna radiation. Cutting straight slits (or slots) on the finite ground plane in vicinity of the antenna was adopted in both [16] and [17]. Apparently current distribution on the ground plane was changed due to the slits and the reduction of mutual coupling was thus achieved. Meanwhile, the radiation pattern of the antenna was also affected through the re-distribution of ground currents. Various diversity techniques along with polarization switching for the improvement of antenna isolations have also been proposed in [18–25]. Among all the approaches, utilization of slits is most cost effective in practical implementations. Yet, care must be taken in the effort of achieving high isolation since redistribution of energy will certainly have effect on the return loss and radiation patterns of the individual antenna elements.

In the following sections, various isolation improvement techniques including planar ground strips, band-notched ground slits, resistive cards between the antenna elements and possible combinations of the above are firstly investigated numerically in Section 2. The key idea is to minimize the mutual coupling between antenna elements without deteriorating too much the performance of individual antennas. Based on the knowledge from Section 2, the design of an antenna system consisting of three loop antennas for WLAN MIMO card bus application will be described in detail in Section III. The designed antenna system will be implemented on a FR-4 substrate with an overall dimension of $48 \times 90\,\mathrm{mm}^2$. The three antennas are spaced side-by-side in a restricted area of $48 \times 30\,\mathrm{mm}^2$, where very strong coupling among them is expected. The electric characteristics, radiation patterns together with over-the-air throughput test results are also included in Section 3 followed by the conclusions in Section 4.
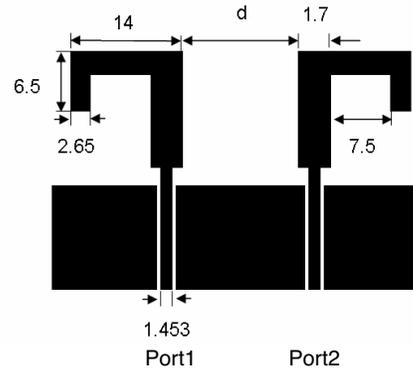
Figure 1. Detailed dimensions of such antennas on a 0.8 mm thick FR-4 substrate with $\varepsilon_r = 4.4$ designed for 2.4 GHz operation. (unit: mm).

2. ISOLATION IMPROVEMENT TECHNIQUES

Potential isolation improvement techniques to reduce the mutual coupling between antennas are firstly numerically examined, which will be later employed in our antenna design for the WLAN MIMO card bus applications. Parametric studies for each case are also performed for completeness purpose. To simplify the analysis without losing generality, two inverted L-shaped monopole antennas with well known characteristics as published in [26, 27], were adopted for investigation. Figure 1 shows the detailed dimensions of such antennas on a 0.8 mm thick FR-4 substrate with $\varepsilon_r = 4.4$ designed for 2.4 GHz operation. The back and front ground sizes are both $48 \times 60\,\mathrm{mm}^2$, with d the spacing between antennas. The outermost dimensions of the antennas together with ground planes were chosen to be exactly the same as the WLAN card ($48 \times 90\,\mathrm{mm}^2$) for practical concerns. A baseline analysis was performed at the extreme case where the two antennas were placed at the maximum separation but remained in the restricted area of $48 \times 30\,\mathrm{mm}^2$. In this case, the spacing d was set at 14.5 mm. The return loss and insertion loss (which is isolation for this case) were simulated to be $S_{11} = -17.52\,\mathrm{dB}$, $S_{22} = -17.27\,\mathrm{dB}$ and $S_{12} = -10.19\,\mathrm{dB}$, respectively using Ansoft HFSS. This isolation should serve as the baseline reference since it exhibited the best value one could get in the restricted area by merely separating the antennas to the maximum distance with no further improvement technique. Possible isolation improvement techniques based on this design were then implemented and discussed in the following subsections.

2.1. Insertion of a Ground Strip Between Antennas

A ground strip was inserted between the antennas on the front side as shown in Figure 2(a), with D being the length of the ground strip. The simulated results of insertion and return losses were also included with D varying in Figure 2(a) and (b). As is observed, the increase in D will subsequently increase the insertion loss, which indicates that a
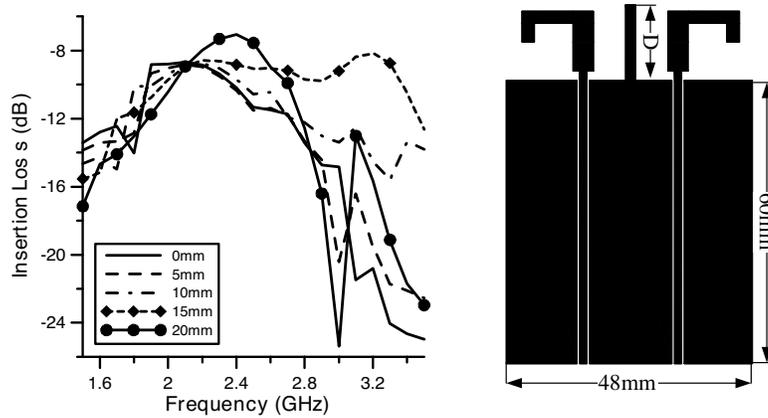
(a)
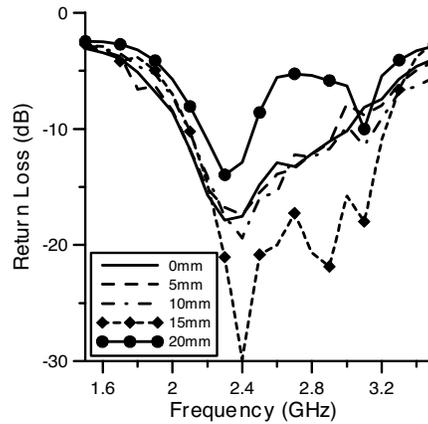
(b)

Figure 2. The (a) insertion and (b) return loss of the antennas with varying D (the length of ground strip) when a ground strip was inserted between the antennas on the front side. The insert in (a) shows the overall dimension of the structure.

stronger mutual coupling is produced. In particular, the insertion loss has been increased to -7.05 dB for the case $D = 20$ mm, a 3 dB increase compared to the baseline case. In spite of the deterioration in isolation with increasing D, the return loss was obviously improved as shown in Figure 2(b). This effect is especially pronounced at $D = 15$ mm where a relatively broadband behavior is observed. A similar behavior was also observed with ground strips inserted on both the front and back sides of ground planes. Conclusively, insertion of ground strips tends to deteriorate the isolation between the antennas yet provides improvesanother freedom for the improvement of the return loss in a broadband sense.

2.2. Cutting a Ground Slot

An effective way of improving isolation between the antennas of this type would be the disturbance of the ground current distribution. Thus, a rectangular slot on the backside of the ground plane was cut for the investigation of the effectiveness of isolation improvement. Figure 3(a) illustrates the location of the slot on the backside of the ground plane with fixed width 1 mm and length D varying. The simulated insertion and return losses are shown in Figure 3(a) and (b), respectively. The improvement in isolation with the existence of the slot is clearly observed. The parametric study results showed that the frequency of minimum insertion loss increases as D decreases, with a minimum of -22.56 dB occurred at 2.4 GHz while D equals 11.5 mm. As is clearly observed from Figure 3(b), this improvement in isolation is at the expense of the narrower bandwidth of the return loss. Additionally, existence of the ground slot tended to push the resonance higher in frequency. Cutting an additional slot on the front side of the ground plane at the exact location as that of the previous case was also investigated. However, the results revealed that the results of double slots were almost exact as those of single slot cut on the back side.

2.3. Ground Slot with Open

Further disturbance on the ground current distribution could be achieved through the addition of an open end on the original slot. The addition of the open end tended to add another discontinuity in the ground current path and was expected to have the band-notch behavior on the overall performance. In this case, both rectangular- and round-shaped open ends were investigated. The original length of the ground slot was set to be 9.5 mm for rectangular-shaped open end and $D = 9$ mm for the round-shaped open end, so that the overall length of the slot was in the vicinity of 11.5 mm which gave the best

(a)

(b)
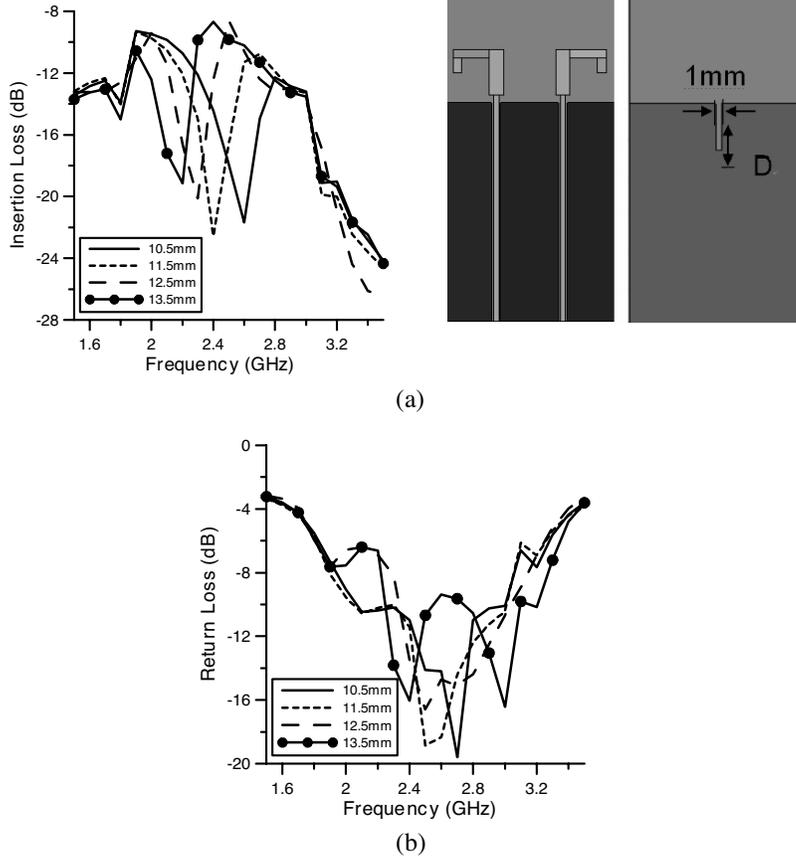
Figure 3. The (a) insertion and (b) return loss of the antennas with varying D (the length of ground slot) when a ground slot was cut from the ground plane on the back side. The insert in (a) shows the overall dimension of the structure.

isolation at 2.4 GHz for the case of uniform ground slot on the backside of ground plane. Figure 4 shows the simulated results for the cases with different widths (rectangular-shaped open end) and diameters (round-shaped open end). It is observed from Figure 4 that the open in the slot end does improve the isolation while the shape does not result in significant impacts. Also a smaller open has a wider bandwidth while a larger open results in a better isolation.

(a)

(b)
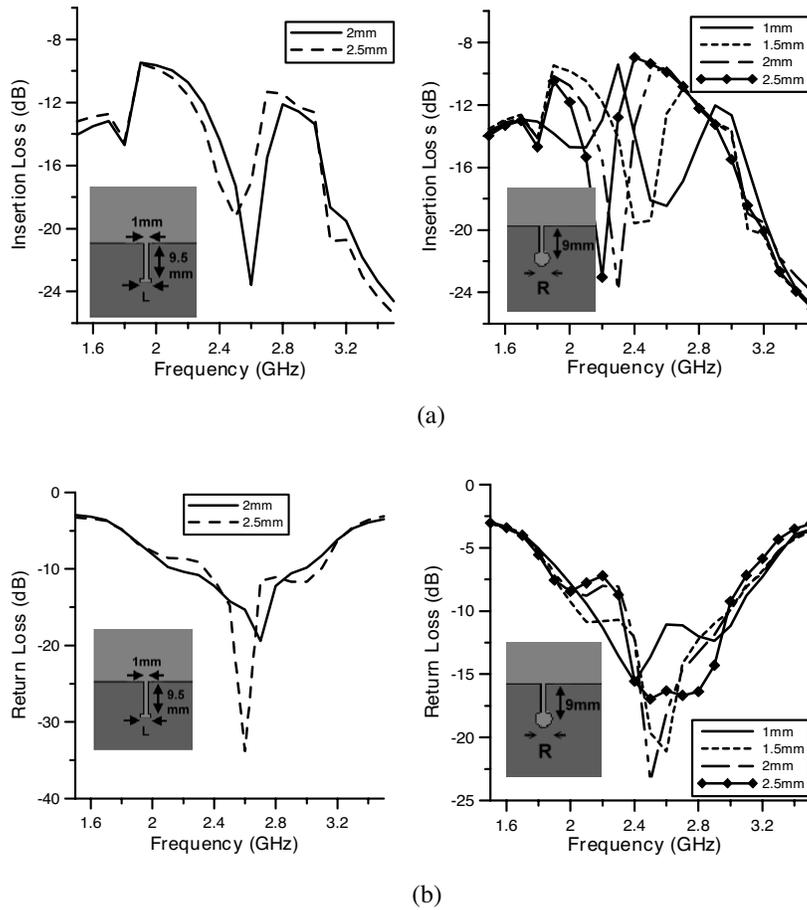
Figure 4. The (a)insertion and (b)return loss of the antennas when a slot with either a rectangular- or a round-shaped open is cut from the backside ground between the antennas. The numbers of length shown in the figures are the values of widths and diameters of rectangular- and round-shaped opens, respectively.

3. ANTENNA DESIGN FOR WLAN MIMO CARD BUS APPLICATION

The characteristics concluded in the previous section indicated that the insertion of ground strips improved the return loss at the expense of increased insertion loss (equivalent to worse isolation). On the contrary, the ground slots have the tendency of isolation improvement

at the expense of worse return loss. These conclusions drawn from numerical simulations inspired the possible combination of proposed techniques to achieve both high isolation and good return loss at the same time.

3.1. Antenna Design

The antenna structure as illustrated in Figure 5 which consisted of three loop antennas fed by coplanar waveguide structure with $1.453\,\text{mm}$ line width was implemented on an FR4 substrate ($\varepsilon_r = 4.4$) of $0.8\,\text{mm}$ thickness. The orientation of the antennas was arranged such that the opening of the middle loop antenna was placed horizontally, which was orthogonal to that of the other two antennas. The main reason for such arrangement was to provide proper diversities for isolation purpose in practical MIMO applications. Insertion of ground strips on the front side between the antennas was implemented with proper adjustment to improve the return loss and enhance the operational bandwidth of the individual antennas. All three antennas as well as the ground strips were printed in the restricted area of $48 \times 30\,\text{mm}^2$ on the FR4 substrate. It is noted that the mutual couplings among these three antennas are much stronger than the situation discussed in Section II, with only two antennas at maximum allowable spacing, since the three antennas are more closely spaced. Minimum requirements of $-10\,\text{dB}$ return loss for individual antennas and $-10\,\text{dB}$ isolation between any two antennas are considered satisfactory for this case. The complete design flow starts with the optimal design for the return losses of individual antennas followed by the improvement in isolations without deteriorating the return losses too much.
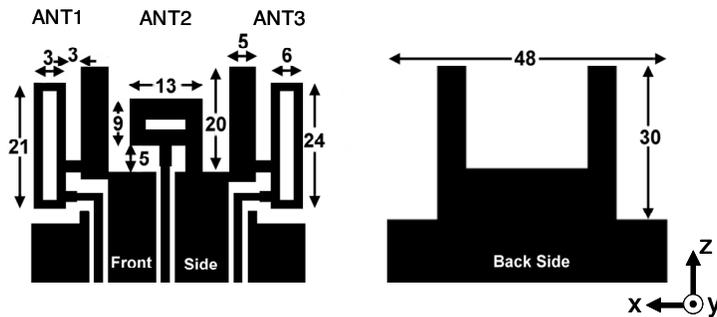
Figure 5. The MIMO antenna structure for WLAN applications. The antennas are numbered as 1, 2 and 3 from left to right. (unit: mm)
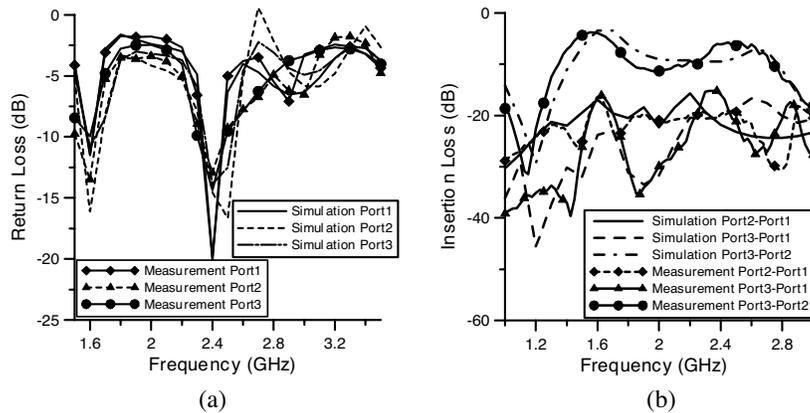
Figure 6. The simulated/measured (a) return and (b)insertion loss of the proposed MIMO antenna structure for WLAN applications.

Figure 6 shows the simulation results of the return and insertion losses of the synthesized design with measurement data included for comparison. As is observed, the measurement results agree very well with simulation and the design is evidently optimized for the best return losses for the three individual antennas shown in Figure 6(a). The insertion losses (isolation), both simulated and measured, between ANT2 and ANT1 (S_{21}), ANT3 and ANT1 (S_{31}) and ANT3 and ANT2 (S_{32}) are shown in Figure 6(b). It is clear that excellent isolation between ANT2 and ANT1 (S_{21}) and ANT3 and ANT1 (S_{31}) at a level of -20 dB at 2.4 GHz is achieved. However, only -6.3 dB isolation is achieved between ANT3 and ANT2 (S_{32}) at 2.4 GHz due to the shorter distance between the terminations of antenna 2 and 3 for such arrangement.

3.2. Isolation Improvement through Ground Slot with Open (T-slot)

To reduce the mutual coupling between ANT3 and ANT2 (S_{32}), a ground slot with rectangular open (T-slot) was implemented on the backside ground plane located at the middle of ANT2 and ANT3 as shown in Figure 7(a). The dimension of this band-notched ground slot was chosen to be 1×17 mm^2 with an optimized 2.5×1 mm^2 open, where the overall length was close to $\lambda/4$ at 2.4 GHz with λ being the wavelength on a FR4 substrate. Such arrangement was expected to result in a nearly $\lambda/2$ propagation path which would make the currents to cancel with the currents directly coupled to the antenna. Figure 7(a)

(a)

(b)
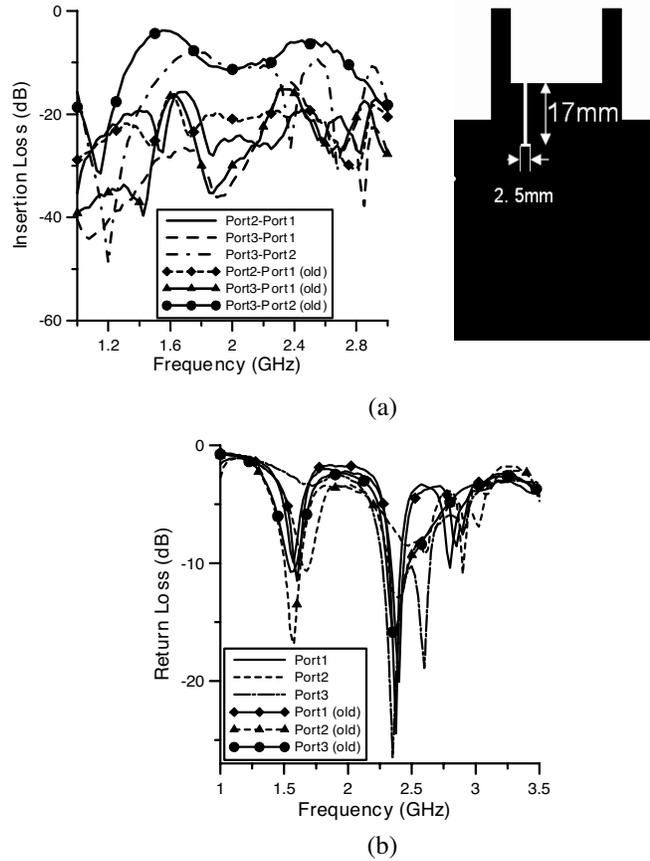
Figure 7. (a) Insertion and (b) return loss of the proposed MIMO antenna with ground slot and rectangular open end inserted on the backside ground between ANT2 and ANT3.

shows the obvious reduction in S_{32} for this case in comparison with the cases without ground slot. It is also observed from Figure 7(a) that the insertion of ground slot between ANT2 and ANT3 did not have significant impact on S_{31} and S_{21}.

In spite of the great improvement in the isolation between ANT2 and ANT3, the deterioration in the return loss on the individual antenna was observed in Figure 7(b). It is clear that the existence of the ground slot has great impact on S_{22} with only -7.67 dB at 2.4 GHz observed. Additional adjustment of the size and locations of the ground strip may result in the return loss improvement according

the conclusions from Section 2. However, in this specific case, the improvements are relatively minor since we are dealing with a very tight allowable area for the three antennas. An alternative yet very effective approach is to use resistive sheets (referred to as R-card hereafter [29, 30]), which will be discussed in the following sub-section.

3.3. Inclusion of an R-card between ANT2 and ANT3

An R-card with a size of $10 \times 15 \, mm^2$ and $5 \, \Omega$ sheet resistance was inserted between ANT2 and ANT3 where the R-card touched antenna 2 at the termination and the ground strip as shown in Figure 8(a). Inclusion of R-card in this manner will potentially reduce the induced currents reflected from the termination, and can thus improve the return loss of the individual antenna. The results of S_{22} and S_{32} are shown in Figure 8(a) and (b), where it is observed that the implementation of R-card has significantly improved the return loss and increased the operation bandwidth. It is noted that the implementation of R-card will cause energy loss because of its resistance and thus minimum extent implementation is required to retain good efficiency. In this design, the minimum length of R-card is adopted such that the return loss meets the $-10 \, dB$ requirement. The insertion loss, S_{32}, does not suffer significantly from this R-card implementation as shown in Figure 8(b). It is evident from the measurement as well as simulation results that combination of T-slot and R-card with optimal ground strip length can achieve the required return loss of individual antennas and isolation simultaneously.

3.4. Radiation Characteristics and Throughput Examinations

The normalized radiation patterns of this MIMO antenna structure are presented in Figure 9(a), (b) and (c) for the patterns at x-y, y-z and x-z planes, respectively, according to the coordinate system shown in Figure 5. In the figure, A1 $\sim$ A3 indicate the patterns of antenna 1 $\sim$ 3 of the original structure while B1 $\sim$ B3 indicate the corresponding cases with isolation improvement techniques implanted as described Section II. It is noted that the patterns on the x-y and x-z planes will certainly have pronounced effect on the mutual coupling between antennas analyzed in this paper. As shown in Figure 9(b), it is clear that the radiation patterns on a y-z plane have not been significantly affected by the implementation of isolation improvement techniques. However, the other two planes have exhibited significant pattern deformations which have resulted in the reduction of mutual coupling between antenna 2 and 3. The radiation characteristics of these antenna designs with
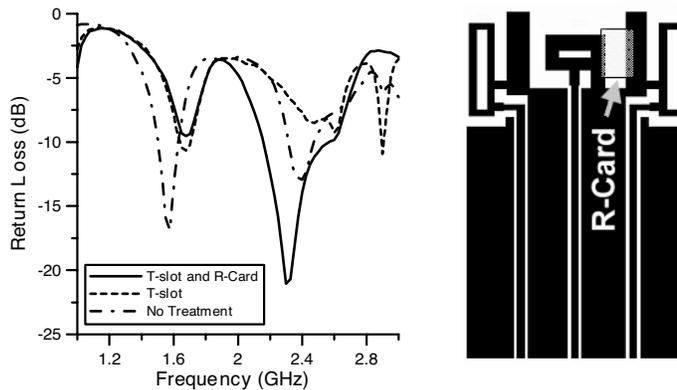
(a)
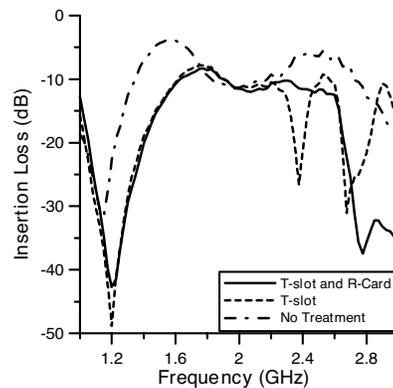
(b)

Figure 8. (a) Return (S_{22}) and (b) insertion (S_{32}) loss of the proposed MIMO antenna structure with both T-slot and R-card implemented to achieve return loss and isolation simultaneously.

and without isolation improvement are summarized in Tables 1 and 2, respectively. Results revealed that a 2 dB enhancement in gains of antenna 1 and 3 were achieved due to implementation of isolation improvement techniques. On the contrary, the gain of antenna 2 is slightly decreased due to the existence of the R-card. The designed antenna structure was tested in a realistic throughput examination between two desktop computers. The antennas were implemented on a 802.11 Access Point (AP) with fixed attenuators of −20 dB to reduce the radiation power so that they can be examined inside a shielding box that has a good isolation of at least −90 dB. The throughput is

(a) *x-y* plane

(b) *y-z* plane

(c) *x-z* plane
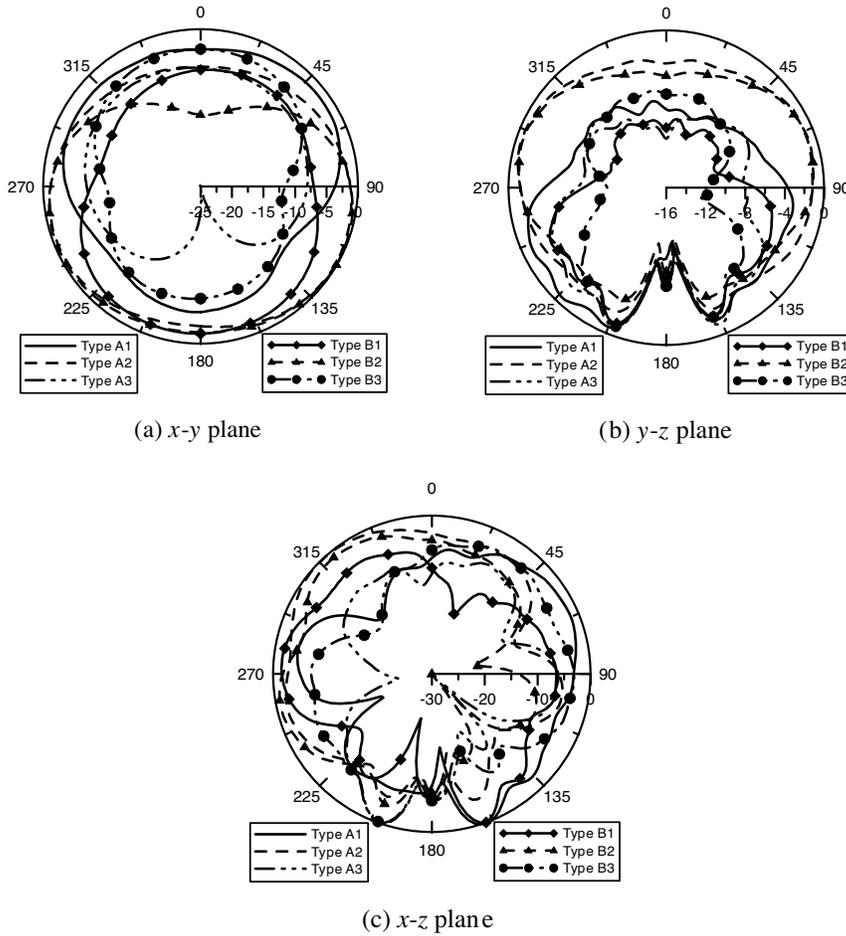
Figure 9. Measured radiation patterns for MIMO antennas with a T-slot/R-card isolation, where A1 ∼ A3 indicate the original antenna structures while B1 ∼ B3 indicate the antenna structure with isolation treatment.

justified by the data transmission rate within 1 minute of time. Three cases of the original antenna structure, the structure with a T-slot and the structure with T-slot and R-card were tested and compared with the results summarized in Table 3. It is clearly observed that the best data transmission rate was achieved for the case of both T-slot and R-card included in the antenna structure, attributing from the excellent return loss and isolation achieved at the same time.

Table 1. Radiation characteristics of antennas without isolation improvement.

Frequency (GHz)	A1		A2		A3	
	Gain (dB)	Directivity (dB)	Gain (dB)	Directivity (dB)	Gain (dB)	Directivity (dB)
2.3	−0.24	6.36	−1.65	3.32	−1.55	6.1
2.35	−3.55	4.58	−1.13	3.17	−0.97	6.13
2.4	−6.42	3.48	−1.25	2.89	−0.97	6.27
2.45	−5.9	4.52	−1.55	2.79	−1.71	6.7
2.5	−6.65	4.23	−1.67	2.7	−2.73	6.9
2.55	−7.01	4.34	−1.54	3.15	−1.23	6.87
2.6	−4.72	5.75	−1.24	3.46	0.16	6.88
2.65	−4.01	6	−1.49	3.73	0.48	6.89
2.7	−2.94	6.11	−1.76	3.69	1.04	6.89
2.75	−0.85	6.98	−2.41	3.81	0.88	6.78
2.8	3.2	8.53	−3.13	4.12	0.43	6.7

Table 2. Radiation characteristics of antenna with isolation improvement.

Frequency (GHz)	B1		B2		B3	
	Gain (dB)	Directivity (dB)	Gain (dB)	Directivity (dB)	Gain (dB)	Directivity (dB)
2.3	1.6	7.64	−2.93	3.16	0.96	6.14
2.35	0.93	7.19	−3.04	3.09	0.81	6.05
2.4	−0.94	6.37	−3.46	2.96	−0.19	5.7
2.45	−3.36	5.89	−3.43	3.16	−0.92	5.75
2.5	−5.21	5.64	−2.91	3.26	−0.95	6.21
2.55	−5.3	6.01	−2.58	3.29	−1.14	6.32
2.6	−4.73	6.33	−1.73	3.85	−0.65	6.11
2.65	−4.89	5.8	−2.34	4.37	0.25	5.98
2.7	−3	5.87	−3.15	3.97	0.18	6.56
2.75	2.01	8.01	−4.8	3.84	−0.51	7.07
2.8	5.07	9.23	−7.75	4.22	0.04	7.83

Table 3. Throughput data summary.

Group	Timing Records Completed	Average (Mbps)	Minimum (Mbps)	Maximum (Mbps)
Original	88	121.156	105.062	139.289
W/T-Slot	94	128.142	113.324	135.754
W/T-Slot & R-card	100	135.579	129.111	148.938

4. CONCLUSION

Various isolation improvement techniques for multiple antenna elements in a closely spaced area have been investigated. While improvement in isolation seemed to have negative impact on the return loss of individual antennas and vice versa, a combination of T-slot, ground strip and R-card has been applied in the design of three loop antennas for MIMO WLAN card bus applications in this paper. Simulation and measurement results have revealed that both return loss and isolation can be simultaneously achieved through optimal design arrangement. Further validation on the data throughput of a practical system also evidenced the superiority of the proposed antenna structure.

REFERENCES

1. Foschini, G. J. and M. J. Gans, "On the limits of wireless communications in a fading environment when using multiple antennas," *Wireless Personal Commun.*, Vol. 6, No. 3, 311–335, March 1998.
2. Usman, M., R. A. Abd-Alhameed, and P. S. Excell, "Design considerations of MIMO antennas for mobile phones," *PIERS Online*, Vol. 4, No. 1, 121–125, 2008.
3. Chen, Y. B., Y. C. Jiao, F. S. Zhang, and H. W. Gao, "A novel small CPW-fed T-shaped antenna for Mimo system applications," *Journal of Electromagnetic Waves and Applications*, Vol. 20, No. 14, 2027–2036, 2006.
4. Li, H.-J. and C.-H. Yu, "MIMO channel capacity for various polarization combinations," *Journal of Electromagnetic Waves and Applications*, Vol. 18, No. 3, 301–320, 2004.

5. Min, K.-S., M.-S. Kim, C.-K. Park, and M. D. Vu, "Design for PCS antenna based on WIBRO-MIMO," *Progress In Electromagnetics Research Letters*, Vol. 1, 77–83, 2008.

6. Gao, G.-P., X.-X. Yang, and J.-S. Zhang, "A printed volcano smoke antenna for UWB and WLAN communications," *Progress In Electromagnetics Research Letters*, Vol. 4, 55–61, 2008.

7. Koo, B.-W., M.-S. Baek, and H.-K. Song, "Multiple antenna transmission technique for UWB system," *Progress In Electromagnetics Research Letters*, Vol. 2, 177–185, 2008.

8. Abouda, A. A. and S. G. Hggman, "Effect of mutual coupling on capacity of MIMO wireless channels in high SNR scenario," *Progress In Electromagnetics Research*, PIER 65, 27–40, 2006.

9. Abouda, A. A., H. M. El-Sallabi, and S. G. Häggman, "Effect of Antenna Array geometry and ULA azimuthal orientation on MIMO channel properties in urban city street grid," *Progress In Electromagnetics Research*, PIER 64, 257–278, 2006.

10. Svantesson, T. and A. Ranheim, "Mutual coupling effects on the capacity of multi element antenna systems," *Proc. IEEE Int. Conf. Acoustics, Speech, and Signal Processing (ICASSP) '01*, Vol. 4, 2485–2488, May 2001.

11. Fredrick, J. D., Y. Wang, and T. Itoh, "Smart antenna based on spatial multiplexing of local elements (SMILE) for mutual coupling reduction," *IEEE Transcation on Antenna and Propagation*, Vol. 52, 106–114, Jan. 2004.

12. Choi, J., V. Govind, and M. Swaminathan, "A novel electromagnetic bandgap (EBG) structure for mixed-signal system applications," *Proc. IEEE Radio and Wireless Conference*, 243–246, Sept. 19–22, 2004.

13. Yang, L., M. Fan, and Z. Feng, "A spiral electromagnetic bandgap (EBG) structure and its application in microstrip antenna arrays," *Proc. IEEE APMC*, Vol. 3, Dec. 4–7, 2005.

14. Fu, Y. Q., Q. R. Zheng, Q. Gao, and G. H. Zhang, "Mutual coupling reduction between large antenna arrays using electromagnetic bandgap (EBG) structures," *Journal of Electromagnetic Waves and Applications*, Vol. 20, No. 6, 819–825, 2006.

15. Ganatsos, T., K. Siakavara, and J. N. Sahalos, "Neural network-based design of EBG surfaces for effective polarization diversity of wireless communications antenna systems," *PIERS Online*, Vol. 3, No. 8, 1165–1169, 2007.

16. Ohishi, T., N. Oodachi, S. Sekine, and H. Shoki, "A method to improve the correlation coefficient and mutual coupling for diversity antenna," *2005 IEEE International Symposium on Antenna and Propagation*, 507–510, 2005.

17. Ren, W., "Compact dual-band slot antenna for 2.4/5 GHz WLAN applications," *Progress In Electromagnetics Research B*, Vol. 8, 319–327, 2008.

18. Khaleghi, A., "Diversity techniques with parallel dipole antennas: radiation pattern analysis," *Progress In Electromagnetics Research*, PIER 64, 23–42, 2006.

19. Tu, T.-C., C.-M. Li, and C.-C. Chiu, "The performance of polarization diversity schemes in outdoor micro cells," *Progress In Electromagnetics Research*, PIER 55, 175–188, 2005.

20. Su, D., D. Fu, T. N. C. Wang, and H. Yang, "Broadband polarization diversity base station antenna for 3G communication system," *Journal of Electromagnetic Waves and Applications*, Vol. 22, No. 4, 493–500, 2008.

21. Kuo, L. C., H. R. Chuang, Y. C. Kan, T. C. Huang, and C. H. Ko, "A study of planar printed dipole antennas for wireless communication applications," *Journal of Electromagnetic Waves and Applications*, Vol. 21, No. 5, 637–652, 2007.

22. Chen, Y. B., T. B. Chen, Y. C. Jiao, and F. S. Zhang, "A reconfigurable microstrip antenna with switchable polarization," *Journal of Electromagnetic Waves and Applications*, Vol. 20, No. 10, 1391–1398, 2006.

23. Mukherjee, P., B. Gupta, and R. Bhattacharjee, "Dual band coplanar microstrip antenna with polarization diversity," *Journal of Electromagnetic Waves and Applications*, Vol. 17, No. 9, 1323–1330, 2003.

24. Kalaye, B. M. B. and J. Rashed-Mohassel, "A broadband and high isolation CPW fed microstrip antenna array," *Journal of Electromagnetic Waves and Applications*, Vol. 22, Nos. 2–3, 325–334, 2008.

25. Hernández-López, M. A. and M. Quintillán-González, "Coupling and footprint numerical features for a bow-tie antenna array," *Journal of Electromagnetic Waves and Applications*, Vol. 19, No. 6, 779–794, 2005.

26. Stutzman, W. L. and G. A. Thiele, *Antenna Theory and Design*, Ch. 2 and Ch. 5, 2nd edition, John Wiley, New York, 1998.

27. Pozar, D. M., "Microstrip antennas," *Proc. IEEE*, Vol. 80, 79–91, Jan. 1992.

28. Wu, D.-J. and H.-T. Chou, "Radiation of a handset monopole antenna in the presence of a finite shielding sheet for the purpose of SAR reduction," *2002 IEEE International Symposium on Antenna and Propagation*, 452–455, 2002.

29. Mahmoud, M. S., T.-H. Lee, and W. D. Burnside, "R-card edge treatment for compact range reflector (2D Case)," *Technical Report727723-14*, The Ohio State University, ElectroScience Laboratory, May 1998.